

DETAILED KINETICS OF A DIFFUSION DRIVEN ADSORPTION PROCESS

Alexandra Ana CSAVDARI^{a,*}

ABSTRACT. The present work completes information reported previously on Chrystal violet adsorption from aqueous solutions onto *Salvinia natans* powder. It identifies intraparticle diffusion as the rate determining step within the sequence of four individual stages of the adsorption mechanism. It also demonstrates, that even is somewhat faster, the film diffusion at the solid-liquid boundary is also slow enough to contribute to the overall process rate. The novel use of a simple kinetic model, consisting of two parallel and competing first-order steps, as well as of an algorithm familiar to pharmacokinetics (the method of residuals), individual rate coefficients of both the film and the intraparticle diffusion were calculated simultaneously from the same kinetic curves. The dependence of their values with employed operating conditions consolidates previous findings and conclusions.

Keywords: Adsorption; Rate determining diffusion; Method of residuals; Competing first-order processes

INTRODUCTION

Adsorption of various organic and inorganic chemical species from gases or wastewaters onto the surface of specially designed solid adsorbents has proved to be highly efficient as well as cost effective. Hence, it has gained increased significance in recent research [1-4]. Within this context, overall process kinetics and mechanism are of outmost importance in the design of any adsorption equipment, which operates either continuously or discontinuously [5-13].

^a Babeş-Bolyai University, Faculty of Chemistry and Chemical Engineering, 11 Arany Janos Street, RO-400028, Cluj-Napoca, Romania

* alexandra.csavdari@ubbcluj.ro



Adsorption experiments follow the process during non-equilibrium, by monitoring its extent as a function of total fluid – solid contact time. The registered parameter is usually an adsorption yield, expressed as a percentage of removed pollutant quantity from its initial amount, or as an adsorption capacity q , expressed in mg pollutant adsorbed by 1g of adsorbent until a certain moment after process initiation. Values are dependent on temperature, pollutant/adsorbent mass ratio [5-13], quality of mixing, pH (for example in dye adsorption [6,8,14]), and of course on the nature of adsorbed as well as adsorbent species. As such, kinetic adsorption models shed light on the rate determining step of the process, hence process mechanism, as well as on the optimum conditions to be employed in order to obtain the desired overall performance. Moreover, adsorption/desorption dynamics knowledge also contribute to the better understanding of catalysis and corrosion phenomena [11].

Dedicated literature [4-5,8-11] usually mentions a succession of four main stages of mass transfer. Each might affect the overall process rate. The first involves the bulk movement of the adsorptive (chemical species to be removed from the fluid) from the bulk phase of the fluid, liquid or gas, to the vicinity of the external surface of the solid adsorbent. This is usually a fast transport that is not taken into consideration when describing adsorption dynamics. On the other hand, the second stage, that of the film diffusion (FD), involving the solute species' crossing of the fluid boundary layer to the actual solid surface, can be much slower and might influence the overall process' rate. The following intraparticle (pore) diffusion stage (IPD), of solute's transport from the surface of the adsorbent into the inner space of its pores, is often mentioned as the rate determining step. The last stage involves the actual adsorption (attachment) of the adsorptive species onto the adsorbent's surface by means of either chemi- or physisorption. This is generally described as happening fast, and hence not affecting the overall adsorption rate.

If the solute's molecule size as well as its initial concentration in the fluid are fairly small, and moreover the mixing quality is low, then the film diffusion is controlling the overall rate. Otherwise, it is usually the intraparticle diffusion [5,9].

Proposed models [5,8-9] describe pseudo-first order or pseudo-second order overall kinetics, take into account only the adsorption or both the adsorption–desorption ensemble of reversible processes, consider diffusion as rate controlling or propose combined diffusion–adsorption control, as well as introduce various non-linear models in order to best fit the experimental data and explain process mechanism [5,9].

Yet, none differentiates between the characteristics (such as rate coefficients) of the film and intraparticle diffusion, nor puts forward values of

both obtained from a single kinetic curve. Moreover, the fact that FD and IPD occur not only successively, but also in parallel (competing), is usually ignored by scientists striving for adsorption dynamics elucidation.

Hence, the main aim of this work is to demonstrate that a simple kinetic model, composed of two parallel and competing first order processes, can be used to describe overall adsorption kinetics in diffusion controlled situations. This implies both rapid bulk movement and chemi-/physisorption, situation easily achieved when toxic organic species (dyes, pesticides, biocides, etc.) are removed from their diluted aqueous solutions by solid high-value inner surface adsorbents [8,12-13]. The model assumes that time resolved non-equilibrium measurements describe in a single kinetic curve both film (FD) as well as intraparticle diffusion (IPD), and hence can be used to determine simultaneously the first-order rate coefficients of both by using the method of residuals (also called Feathering or Peeling method). This is a consecrated data processing procedure, which uses a biexponential equation to describe administrated drug pharmacokinetics, when distributed between the central and the peripheral compartments [15-16].

Experimental data used to demonstrate this novel approach were provided by the authors of a previous study [14]. This compared the phytoremediation performances of living and powder *Salvinia natans* (SN) in the removal of Crystal violet (CV) from its aqueous synthetic solutions. In both cases, dynamic behavior was described by an overall second-order process and cumulative corresponding rate coefficients have been calculated.

Yet, no distinction has been presented among the individual stages in the case of powder *S. natans*, a process which matches a usual S-L adsorption. In other words, no explanation has been given about the identity of the rate determining process as well as about the values of its rate coefficients. Final conclusions mentioned that adsorption of CV on powder SN proved to be physical in nature, but did not prove whether it is slow or fast as compared to the diffusion driven film and intraparticle steps.

Therefore, this work also aims to complete the conclusions of the former study for the case of Crystal violet adsorption on powder *Salvinia natans*, by: (1) identifying the rate determining step, (2) putting forward values for the rate coefficients of individual stages of the process, and (3) completing and consolidating the previous study's conclusions by interpreting the newly found rate coefficients' dependence on employed experimental conditions. As stated above, goal (2) is achieved by using an ensemble of two parallel (competing) first-order processes and the method of residuals to calculate both FD and IPD rate coefficients from kinetic curves describing the overall residual CV concentration *versus* total S-L contact time.

RESULTS AND DISCUSSION

Validity of the rate determining intraparticle diffusion assumption

Published experimental results describing Crystal violet adsorption from its aqueous solution on *Salvinia natans* powder [14] rely on kinetic curves representing the adsorption capacity q (mg CV / g SN powder) as a function of total contact time t (min, h). Data were collected at various temperatures (10, 23, 35 and 40°C, respectively) and at variable initial concentration of CV, in the range of 20 to 90 mg/L. Hence, by keeping the same amount of solid SN powder, the adsorptive/adsorbent mass ratio has been varied. The effects of rotation speed and aqueous environment pH value on the process were also assessed.

Since the possibility of the IPD to be the rate determining step has not been explored, the linearity of adsorption capacities at a given time (q_t) plots *versus* the square root of total contact time ($t^{0.5}$) has been checked. According to literature [8-11], a linear dependence - such as the one described by equation (1) - demonstrates that pore diffusion is the slowest stage of the entire adsorption process.

The slope k_{IPD} ($\text{mg}\cdot\text{g}^{-1}\cdot\text{h}^{-0.5}$) stands for the intraparticle diffusion rate coefficient. Such plots may present multi-linearity [6-7], which indicates that two or more rate controlling steps occur during the course of the overall process. In these cases, each slope stands for a different k_{IPD} value, characterizing pores of different diameters. Smaller pores are described by lower k_{IPD} values, since the path available for diffusion also becomes smaller [6-7, 17].

The **intercept** in equation (1) also helps in the assessment of the diffusion's role in the overall process. It is correlated with the thickness of the boundary layer, and as such with the importance/significance of film diffusion [7]. If the plot is linear and the intercept is equal to zero (the plot passes through the origin), then only IPD is significant. If the intercept differs from zero (the plot does not pass through the origin), then FD plays an observable role in the overall process, and its contribution to the overall adsorption rate cannot be ignored. The higher the intercept's value, the more significant the FD gets.

$$q_t = k_{IPD} t^{0.5} + \text{intercept} \quad (1)$$

Figure 1 illustrates an example of q_t vs $t^{0.5}$ plot, for the data presented by Mânzatu *et al.* [14]. The linearity is proven by the good correlation coefficient. Moreover, there is no observable multilinearity and the line does not pass through the origin. Hence: (i) IPD is rate determining, but (ii) FD cannot be ignored in the overall rate, and (iii) the pore size of the SN powder appears to be uniform.

Similar results were obtained for all employed experimental conditions described in [14]. Variation of the initial CV concentration of the aqueous media, $[CV]_0$, between 30-90 mg/L, but by keeping all other experimental conditions unchanged (see Figure 1), causes no significant change in the rate constant k_{IPD} . Its value remains $4.83 \pm 0.93 \text{ mg.g}^{-1}.\text{h}^{-0.5}$, suggesting that IPD occurs in similar sized pores. The rate coefficient of IPD does not change with increasing $[CV]_0$, yet the overall rate does, because the FD gets to be more significant in the sum of both. This is suggested by the fact that the intercept of equation (1) increases proportionally with the value of $[CV]_0$, from 2.48 mg/g to 19.53 mg/g. In other words, internal diffusion is rate determining within the overall process, yet a higher dye concentration in the bulk will amplify the driving force of diffusion, hence its rate, but not its rate coefficient.

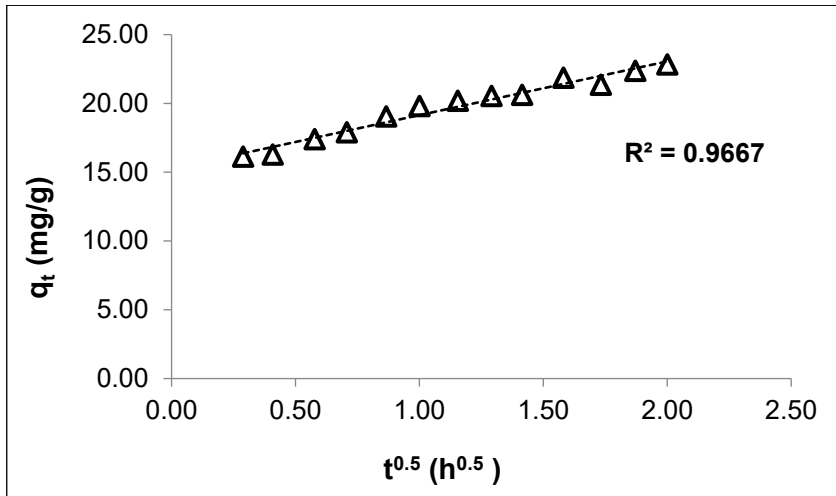


Figure 1. Testing the validity of rate determining IPD assumption, by means of the q_t vs $t^{0.5}$ plot. ($[CV]_0 = 50 \text{ mg/L}$; $m_{SN} = 0.40 \text{ g}$; $\text{pH} = 5.4$; 23°C ; 9000 rot/h)

By changing the temperature between 10 and 40°C under the same operating conditions (see Figure 1), the values of k_{IPD} average around $11.94 \pm 1.54 \text{ mg.g}^{-1}.\text{h}^{-0.5}$ with some minor deviation. The thickness of the boundary layer, correlated to the intercept of equation (1), will result in a value of $3.11 \pm 1.38 \text{ mg/g}$. Variability of these values is low and exhibits no trend; thus it may be due to measurement errors. Hence, temperature does not affect significantly the diffusion driven processes, at least not within this narrow variation domain.

The same conclusions may be drawn for variable pH, within the range of 3.35 to 10.00 units. k_{IPD} averages around $11.25 \pm 1.41 \text{ mg} \cdot \text{g}^{-1} \cdot \text{h}^{-0.5}$, while the intercept around $3.25 \pm 0.93 \text{ mg/g}$. Both values are very close to the ones calculated for the temperature dependence. Thus, neither parameter affects the rates of FD and IPD.

It may be concluded that rate determining intraparticle diffusion has been proved. Film diffusion may not be ignored, yet it is somewhat faster. Even though equation (1) is able to offer some information related to the contribution of diffusion to the overall process rate, it cannot provide the individual rate coefficients of FD and IPD, respectively.

Simultaneous determination of individual rate constants for both film and intraparticle diffusion steps

In order to overcome this shortcoming, this paper proposes the following:

- The overall process is described by an ensemble of two competing, rate determining, first-order steps (I and II, respectively), namely the FD and the IPD, as shown in Figure 2. ED stands for the “external” film diffusion and IPD for the “internal” pore diffusion. k_1 and k_2 , respectively, stand for the first order rate coefficients of the two parallel competing stages.
- Even though IPD is succeeding ED, it is much slower, hence the bulk of the CV transport in step I is carried out *via* ED.
- ED is faster than IPD ($k_1 > k_2$)
- The overall adsorption rate may be written as the disappearance rate of CV from the aqueous bulk phase, and further as the sum of the rates of steps I and II, as it is expressed by equation (2).
- The adsorption is occurring immediately as the CV molecule reaches the adsorption’s active site.

$$r = -d[CV]/dt = r_I + r_{II} = k_1 [CV] + k_2 [CV] \quad (2)$$

Simple chemical kinetics formalism will transform equation (2) into a sum of two exponential terms:

$$[CV] = A \exp(-k_1 t) + B \exp(-k_2 t) \quad (3)$$

In equation (3), A and B represent the amount of initial CV quantity theoretically corresponding to removal solely by film or intraparticle diffusion, respectively. Their sum should ideally be equal to $[CV]_0$.

DETAILED KINETICS OF A DIFFUSION DRIVEN ADSORPTION PROCESS

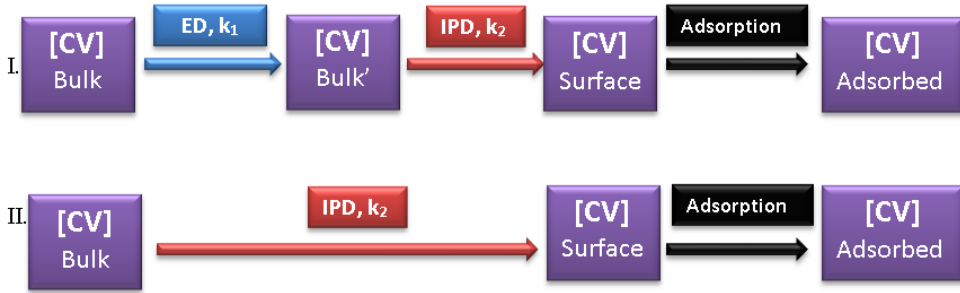


Figure 2. Kinetic model proposed to determine the individual rate coefficients of film and intraparticle diffusion, respectively.

At the initiation of the process when total contact times are short and $t \rightarrow 0$, the rate r_{I} of the ED is significantly higher than the rate r_{II} of IPD, thus r_{II} may be neglected in equation (2). Hence,

$$[CV] \approx A \exp(-k_1 t) \quad (4)$$

In advanced phases of the process when $t \rightarrow \infty$, the situation reverses and r_I may be neglected. Hence,

$$[CV] \approx B \exp(-k_2 t) \quad (5)$$

The method of residuals [15-16] is designed to enable the calculus of both k_1 and k_2 values from a single kinetic curve, provided that: (i) there is a sufficient difference between their values, so that the assumptions in equations (4) and (5) are true, and (ii) there are sufficient [CV] vs t experimental data pairs. Both conditions are satisfied in this case. The calculus algorithm is detailed in the experimental section.

Table 1 summarizes the results. It may be concluded that both k_1 and k_2 increase gradually with temperature. This may indicate a slight endothermic behaviour [8]. Also, the solubility of the CV dye decreases with increasing temperature, hence minimizing the effect of desorption [14].

The activation energy of both film and intraparticle diffusion may be calculated by means of Arrhenius linearization $\ln(k)$ vs $1/T$. In both cases good correlation coefficient lines were obtained: $R^2 = 0.9354$ for k_1 values and $R^2 = 0.9007$ for k_2 values, respectively. The slopes generated activation energies of 10.35 and 2.86 KJ/mole for the FD and IPD processes. These values are in agreement with those generally listed for physical phenomena, IPD being usually less sensitive to temperature changes.

Table 1. Values of the individual film (k_1) and intraparticle (k_2) diffusion process rate coefficients, as a function of operating parameters

| Temperature (°C) | [CV] ₀ (mg/L) | Mixing rate (rot/h) | pH | k_1 (1/h) | k_2 (1/h) |
|------------------|--------------------------|---------------------|-------|-------------|-------------|
| 10 | 50 | 9000 | 5.40 | 0.962 | 0.343 |
| 23 | | | | 1.052 | 0.375 |
| 35 | | | | 1.313 | 0.378 |
| 40 | | | | 1.468 | 0.390 |
| 23 | 30 | 9000 | 5.40 | 1.561 | 0.147 |
| | 40 | | | 3.909 | 0.176 |
| | 50 | | | 3.377 | 0.279 |
| | 70 | | | 3.142 | 0.148 |
| | 90 | | | 2.891 | 0.233 |
| 23 | 30 | 9000 | 5.40 | 3.122 | 0.115 |
| | | 15000 | | 3.041 | 0.115 |
| | | 18000 | | 2.188 | 0.106 |
| 23 | 50 | 9000 | 3.35 | - | 0.300 |
| | | | 5.40 | | 0.286 |
| | | | 7.30 | | 0.461 |
| | | | 8.62 | | 0.448 |
| | | | 10.00 | | 0.305 |

Altering the dye's initial concentration should not affect the rate constants of diffusion, but alters the rates *via* modifying the value of its driving force: the concentration difference between the bulk and the surface values, respectively. Values in Table 1 show however a certain scattering, probably due to experimental and calculus errors (only a few concentration vs time data are available for the determination of each rate coefficient value). Averages of $k_1 = 2.975 \pm 0.876 \text{ h}^{-1}$ and $k_2 = 0.197 \pm 0.058 \text{ h}^{-1}$ have been calculated.

Table 1 suggests that high mixing rates result in a slight lowering of both k_1 and k_2 . This might be caused by the mechanical instability of the solid adsorbent (dried and milled plant leaves). At high speed, the stirrer crushes most probably the adsorbent, hence lowers somewhat its pore dimensions. As a result, diffusion slows down.

In case of experiments carried out at various pH of the aqueous media, the data enabled only the calculus of k_1 . The highest value corresponds to 7.3 pH. Crystal violet is a basic dye; consequently under acidic conditions

hydrogen ions inhibit the binding of positively charged Crystal violet ions to the surface of the sorbent [8, 14].

CONCLUSIONS

This work completes the conclusions of a previously reported study on Crystal violet adsorption dynamics onto powder *Salvinia natans*. Although the authors propose a pseudo-second order rate law which fits well the experimental data, this does not provide information regarding the process mechanism, since it treats it as a single generic process.

Hence, by looking at the individual stages of the process, by identifying the rate determining step as being the intraparticle diffusion, and by also demonstrating that the film diffusion's contribution to the overall rate is not negligible, the present paper sheds more light upon the removal mechanism of various organic dyes from their aqueous solutions by means of adsorption.

Moreover, the treatment of the process as an ensemble of two competing first-order processes (the film and the intraparticle diffusion respectively), as well as the novel use of a time-resolved data processing approach, borrowed from the field of pharmacokinetics, enabled the simultaneous determination of both slow diffusion process rate coefficients. Their dependence as a function of operating conditions (temperature, initial CV concentration, mixing rate and pH) is in agreement with previous conclusions [14], yet completes and consolidates them.

EXPERIMENTAL SECTION

Calculus was carried out by using *Microsoft Excel*. Experimental data Chrystal violet concentration *versus* total S-L contact time, under various operating conditions, were provided by the authors of work described in reference [14].

The calculus algorithm of the method of residuals contains the steps below [15]. The principle of the method is also illustrated in Figure 3.

- Logarithm values of [CV] are plotted against the contact time t .
- At high contact times the graph reaches linearity. The slope of this line gives the value of k_2 . The value of B in equation (5) corresponds to its intercept.
- The equation of this line (corresponding to the linearized form of equation 5) is further used to calculate the differences between y-coordinate values on the Crystal violet concentration-time plot and

the y-coordinate values from the extrapolated line. These values correspond to the residuals – see Figure 3.

- The logarithm values of residuals are plotted versus their corresponding contact time (close to the beginning of the process).
- A new line is generated that corresponds to the linearized form of equation 4. Its slope stands for k_1 and its intercept for A in equation (4), respectively.

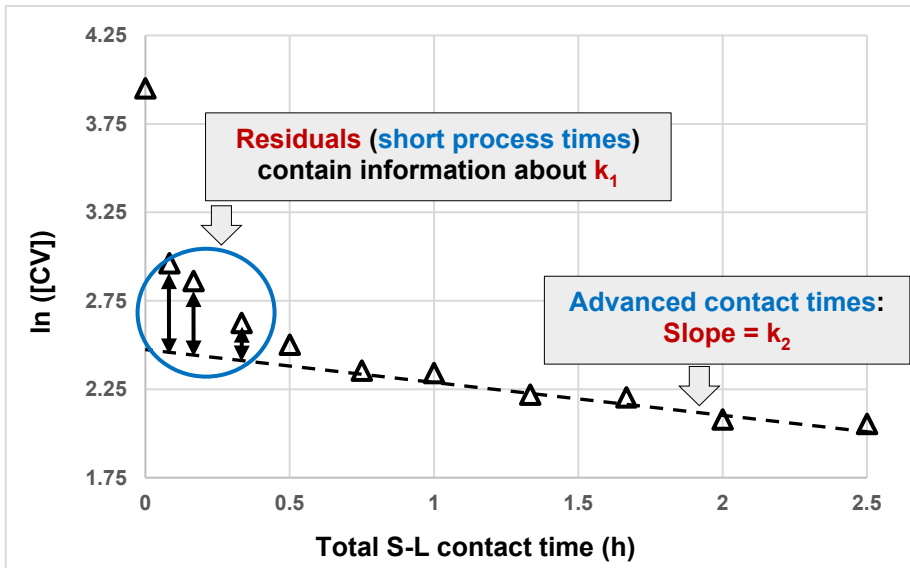


Figure 3. Illustration of the method of residuals for the calculus of both individual film (k_1) and intraparticle (k_2) diffusion process rate coefficients from a single kinetic curve. Experimental conditions are those listed for Figure 1.

REFERENCES

1. V. Krstić; Role of zeolite adsorbent in water treatment. In *Handbook of Nanomaterials for Wastewater Treatment: Fundamentals and Scale up Issues*, Bh. Bhanvase, Sh. Sonawane, V. Pawade, A. Pandit (Eds.); Elsevier, Amsterdam, The Netherlands, **2021**, Chapter 14, pp. 417-481.
2. T. R. Sahoo, B. Prelot; Adsorption processes for the removal of contaminants from wastewater: the perspective role of nanomaterials and nanotechnology. In *Nanomaterials for the Detection and Removal of Wastewater Pollutants*, B. Bonelli, F. S. Freyria, I. Rossetti, R. Sethi, (Eds.); Elsevier, Amsterdam, The Netherlands, **2021**, Chapter 7, pp. 161-222.

3. H. K. Agbovi, L. D. Wilson; Adsorption processes in biopolymer systems: fundamentals to practical applications. In *Natural Polymer-Based Green Adsorbent for Water Treatment*, Elsevier, S. Kalia (Ed.), Amsterdam, The Netherlands, **2021**, Chapter 1, pp. 1-51.
4. T. A. Saleh; *Kinetic models and thermodynamics of adsorption processes: Classification*. In *Surface Science of Adsorbent and Nanoadsorbents*, T. A. Saleh (Ed.), Elsevier, Amsterdam, The Netherlands, **2022**, Chapter 3, pp. 65-97; *Series Interface Science and Technology*, **2022**, 34, 65-97.
5. K. L. Tan, B. H. Hameed, *J. Taiwan Inst. Chem. Eng.*, **2017**, 74, 25-48.
6. G. F. Malash, M. I. El-Khaiary, *J. Colloid Interface Sci.*, **2010**, 348, 537-545.
7. R. Ocampo-Pérez, J. Rivera-Utrilla, C. Gómez-Pacheco, M. Sánchez-Polo, J. J. López-Penalver, *Chem. Eng. J.*, **2012**, 213, 88-96.
8. M. T. Yagub, T. K. Sen, Sh. Afroze, H. M. Ang, *Adv. Colloid Interface Sci.*, **2014**, 209, 172-184.
9. H. Qiu, L. Lv, B-C. Pan, Q-J. Zhang, W-M. Zhang, Q-X. Zhang, *Zhejiang Univ. Sci. A.*, **2009**, 10(5), 716-724.
10. L. Largitte, R. Pasquier, *Chem. Eng. Res. Des.*, **2016**, 109, 495-504.
11. S. Azizian, *J. Colloid Interface Sci.*, **2004**, 276, 47-52.
12. A-M. Danciu, A. Csavdari, *II. International Agricultural, Biological & Life Science Conference*, Edirne, Turkey, **2020**, Abstract Book, pp. 288.
13. A-M. Danciu, A. A. Csavdari, *5th International Conference on Chemical Engineering*, ICCE, Iași, Romania, **2020**, Abstract Book, pp. 95.
14. C. Mânzatu, B. Nagy, A. Török, L. Silgahi-Dumitrescu, C. Majdik, *Studia UBB Chemia*, **2015**, 60(4), 289-304.
15. S. E. Leucuța, *Biofarmacie și Farmacocinetică*, Editura Dacia, Cluj-Napoca, **2010**, pp. 171-235.
16. <https://www.intechopen.com/chapters/63161>
17. F-Ch. Wu, W-R. Tseng, R-Sh. Juang, *Chem. Eng. J.*, **2009**, 153, 1-8.